Adsorption of poly(methacrylic acid) onto differently charged silica nanoparticles and its consequences on particles clustering

Clément Robin, Cédric Lorthioir, Azad Erman, Javier Perez, Abdoulaye Fall, Guillaume Ovarlez, Catherine Amiel, Clémence Le Coeur

Adsorption of poly(methacrylic acid) onto differently charged silica nanoparticles and its consequences on particles clustering.

Authors:

Clément Robin [a], Cédric Lorthioir [b], Azad Erman [a], Javier Perez[c] , Abdoulaye Fall [d], Guillaume Ovarlez [e], Catherine Amiel [a] *, Clémence Le Cœur [a, f]

Affiliations:

(a) Univ Paris Est Creteil, CNRS, ICMPE, UMR 7182, 2 rue Henri Dunant, 94320 Thiais, France

(b) Sorbonne Université, CNRS, Laboratoire de Chimie de la Matière Condensée de Paris, 4 Place Jussieu, 75005 Paris, France

(c) Soleil Synchrotron, Gif-sur-Yvette, France

(d) Laboratoire Navier (UMR 8205), CNRS, Ecole des Ponts ParisTech, Univ. Gustave Eiffel Cité Descartes-77420 Champs sur Marne, France

(e) Univ. Bordeaux, CNRS, Solvay, LOF, UMR 5258, F-33608 Pessac, France

(f) Laboratoire Léon Brillouin, CEA-CNRS (UMR-12), CEA Saclay, Université Paris-Saclay, 91191 Gif-sur-Yvette Cedex, France

Corresponding Author : Catherine Amiel [a], email: amiel@icmpe.cnrs.fr

Highlights

- Poly(methacrylic acid) adsorption was studied on three differently functionalized silica nanoparticles, at 3 pH.
- Adsorption was stronger at pH3 and much larger for the amine functionalized silica.
- Nanoparticle clustering was well correlated to the strength of the polymer /silica interactions.

Abstract

This work aims at gaining a comprehensive picture of the interactions between three differently functionalized silica nanoparticles and a polyacid – PMAA namely – in aqueous media. Native silica nanoparticles and silica nanoparticles functionalized with amine or quaternary amine groups are either negatively or positively charged with various charge densities whereas PMAA chains display an increasing negative charge density as the pH is increased from 3 to 9. Adsorption isotherms were obtained by Total Organic Carbon (TOC). It was shown that native silica interacts only weakly with PMAA while stronger adsorptions were evidenced for the two amine-functionalized silica. Whereas electrostatic attractive interactions between positively-charged surfaces and negatively-charged PMAA are driving the adsorption at pH larger than 3, hydrophobic interactions between the propyl moieties of the grafts at the silica surfaces and the methyl groups of the PMAA hypercoils are dominating at low pH value. In this last case, the more hydrophobic the silica surface is, the higher the adsorption. Contrary to expectations, hydrophobic interactions (dominating at low pH) seem to be stronger than attractive electrostatic interactions (dominating at pH larger than 3) as adsorbed amounts are larger in the first case. Small-angle X-ray scattering experiments were performed on PMAA/silica dispersions under the condition of saturation adsorption in order to correlate the extent of particle dispersion with polymer/surface interactions. The stronger the polymer/surface interactions, the more compact aggregates are formed.

Keywords: Poly(methacrylic acid); adsorption; silica nanoparticles; small angle x-ray scattering

Introduction

The ability of polyelectrolytes to tune surface interactions and colloidal stability is of prime importance in a large variety of industrial processes such as papermaking[1] , wastewater treatment[2] or biomedical applications.[3, 4, 5] This is the interplay between polymer/surface interactions and particle/particle interactions which is at the origin of the microstructures of the polymer / nanoparticle dispersions and of their stability.

Polyelectrolyte adsorption onto colloidal surfaces has been the focus of many experimental investigations, theoretical studies, based on random sequential adsorption models, or self-consistent approaches, as well as numerical works, based on computer simulations. [6, 7, 8, 9] Whereas highly-charged polyelectrolytes are expected to adsorb strongly on surfaces of opposite charge, it is known that non-electrostatic interactions are also at play in the adsorption mechanism. This is particularly true in the case of weak polyelectrolytes such as polyacids which display residual adsorption even when the surfaces are negatively charged. Such a behaviour has been reported for the adsorption of poly(acrylic acid) (PAA) onto SiO_2/ TiO_2 nanoparticles,[10] [11] or onto SiO_2. [12]

As with PAA, poly(methacrylic acid) (PMAA) has a pH-dependent ionization degree (α).[13–17] It should be noticed that these changes in the ionization degree are responsible for significant conformational changes of the PMAA chains. Unlike PAA for which the coils extend regularly with increasing α, a transition from hypercoiled conformation (at low α or low pH) to extended random-coil conformation (at large α or large pH) occurs around $\alpha_c = 0.22$ (pHc = 5.5). Indeed, the presence of the methyl groups in PMAA is responsible for the collapse of the PMAA chains at low pH. These globules are maintained until α reaches α_c, the threshold above which the electrostatic interactions overcome the intramolecular forces (hydrogen bonding and hydrophobic interactions). pH-responsive adsorption of PMAA onto hematite nanoparticles has been reported, as polymers bear pH-dependent charges and hematite particles are positively charged within the pH range 3 - 9. Adsorbed amounts as high as 2.1 mg/m^2 were obtained but these values were strongly influence by the pH and the PMAA molecular weight.[18]

In the field of colloid science, silica nanoparticles occupy a prominent position because of their easy preparation, the good control of their size and their low toxicity. Moreover, their surface modification by organic molecules is well documented. As silica surfaces are negatively charged for pH between 3 and 9, their functionalization with amine groups has been the focus of several studies in order to inverse the surface charge in this pH range.[12, 19]

The aim of this work was to gain a comprehensive picture of the interactions between 3 differently charged silica particles and a polyacid, PMAA. Native silica nanoparticles and silica nanoparticles modified with amine or quaternary amine groups respond differently to pH whereas PMAA chains bear increasing density of negative charges as the pH is increased from 3 to 9. The pH will thus trigger the interactions between the polymer chains and the colloidal

surfaces. A particular attention was paid to the correlation between the pH-triggered conformational properties of PMAA and its adsorption behavior on the one hand and on the surface chemistry of the silica particles on the other hand. For this purpose, these systems were investigated by TOC measurements for the adsorption isotherms, zeta potential measurements and small-angle X-ray scattering.

Materials and Methods

Materials.

Ludox® LS colloidal silica was purchased from Sigma-Aldrich France. Their nominal diameter and specific surface area 12 nm and 215 m^2/g. (3-aminopropyl)trimethoxysilane and 3-(trimethoxysilyl)propyl-N,N,N-trimethylammonium were purchased from Sigma-Aldrich France and Gelest Pennsylvania USA, respectively. Prior to use, the concentrated silica dispersions were diluted (100 g/L) and dialyzed against water to remove traces of stabilizing compounds. The pH of the suspensions was around 8.

Poly(methacrylic acid) was purchased from Polymer Science Inc. (sample 1) and from Sigma-Aldrich France (sample 2). The molar mass and molar mass distributions were obtained using size exclusion chromatography (SEC). Prior to analysis, the polymers were modified by methylation of the carboxylic acid group using trimethylsilyldiazomethane.[20] The samples were analyzed in tetrahydrofuran at a concentration of 10 mg/mL and a temperature of 25°C. The column used was a polystyrene mixed C13 column for organic solvents. The setup was equipped with a refractive index detector (RI) at 930 nm and a light scattering detector. From this experiment, the average molar masses (M_n and M_w) and the polydispersity (Đ), corresponding to M_w/M_n, were derived from the RI signal using a calibration curve of poly(methyl methacrylate) standards purchased from Polymer Laboratories. The results are shown in Table 1.

Table 1: Characteristics of the PMAA polymers

PMAA sample	M_w (kg/mol)	M_n (kg/mol)	Đ
1	451	372	1.2
2	21.6	18.5	1.17

Silanization of silica nanoparticles. According to a method described in the literature,[19] Ludox® LS colloidal silica nanoparticles have been chemically modified in order to graft either

amine terminal groups or quaternary amine groups. Typically, for the $SiNH_2$ particles, 6 g of ludox LS suspension (30%) was diluted in 30 mL ultrapure water and the solution was sonicated for 15 minutes. Reagent solution was prepared by adding 2.1 mg of reagent (3-aminopropyl)trimethoxysilane) to 24 mL ultrapure water and it was mixed to the particle dispersion under strong stirring. The PH was then adjusted by adding HCl 1M until a value close to 5. Then the reaction was conducted at 60°C under stirring and reflux during 18 h. At the end, the dispersions are dialyzed against ultrapure water during 48 h. For the Si-TMA particles, the process was identical except for the first step which was as follows: 6 g of ludox LS suspension (30%) was diluted in 54 mL ultrapure water and the solution was sonicated for 15 minutes. Then 6.4 mL reagent (3-(trimethoxysilyl)propyl-N,N,N-trimethylammonium) was added to the particle suspension under strong stirring. In the following, the 3 different kinds of silica nanoparticles will be denoted as SiOH (native nanoparticles), $SiNH_2$ (amine-functionalized nanoparticles) and Si-TMA (quaternary amine-functionalized nanoparticles). The silica thus modified were characterized by thermogravimetric analysis (TGA) and solid-state NMR. Prior to analysis, the samples were dried under reduced pressure overnight at 50°C for TGA and, in the case of NMR measurements, kept during 72 h at 80°C in order to eliminate residual water. TGA measurements (TA instrument) were performed from 20 to 800 °C in air at a heating rate of 20 °C/min.

Solid-state NMR. Solid-state NMR experiments were performed on a Bruker Avance III 400 MHz wide-bore NMR spectrometer, with a 4 mm magic-angle spinning (MAS) double-resonance probehead. The ^{13}C (^{29}Si) solid-state NMR spectra were acquired using $^{1}H \rightarrow {}^{13}C$ ($^{1}H \rightarrow {}^{29}Si$) cross-polarization experiments, carried out with a MAS spinning frequency of 5 kHz. The 90°(^{1}H) pulse length was equal to 3.6 μs, the ^{1}H radio-frequency field during the $^{1}H \rightarrow {}^{13}C$ ($^{1}H \rightarrow {}^{29}Si$) magnetization transfer was optimized and fixed to 79 kHz (44 kHz) while the contact time was set to 1 ms (^{13}C) and 5 ms (^{29}Si). The SPINAL-64 scheme was used for the ^{1}H dipolar decoupling applied during the detection of the ^{13}C (^{29}Si) NMR signal, with a decoupling strength of 69 kHz. The recycle delay was adjusted according to the $T_1(^{1}H)$ relaxation and set to 5 s. The ^{13}C (^{29}Si) chemical shift values were referenced to tetramethylsilane (TMS) using a secondary standard: glycine for ^{13}C NMR (δ = 176.0 ppm for the carbonyl carbon from α-glycine) and Hectorite for ^{29}Si NMR (δ = -96.0 ppm for the Q^3 sites from Hectorite).

Adsorption isotherms. Adsorption isotherms of PMAA on the 3 different kinds of silica particles were determined at pH equal to 3, 6 and 9. Samples with a given amount of silica (12.5 g/L) and an increasing amount of PMAA were prepared and the pH was adjusted using 0.1 M HCl and NaOH solutions. These samples were equilibrated at 20°C for 24 hours under mild stirring and then, centrifuged at 40000 rpm for 1 h, using an ultracentrifuge from Beckman Coulter (Optima Max-XP, type TLA 110 rotor). The supernatant was carefully collected and its polymer concentration was determined from Total Carbon Analyses (TOC), carried out with a Shimadzu TOC-L CSN instrument, which was calibrated by a potassium hydrogen phthalate solution in ultrapure water (2.125 g dm^{-3} corresponding to 1000 mgC dm^{-3}) and tested with free PMAA solutions. The amount of adsorbed polymer was deduced from the difference between the initial and equilibrium concentrations of the polymer.

Zeta potential. Zeta potentials of the silica dispersions (2 g/L), NaCl 0.01 M, with or without PMAA (1 g/L) were determined at 20°C, for pH varying between 3 and 9. These measurements were performed on a Zetasizer Nano-ZS (Malvern Instrument) equipped with a He-Ne laser (λ = 633 nm). The zeta potential was derived from the electrophoretic mobility using the general Smoluchowski equation.[21]

SAXS. SAXS experiments have been performed on the SWING beam-line at SOLEIL, France and on Xeuss 2.0 SAXS instrument of IRAMIS\SWAXS Lab in CEA Saclay. For the measurements performed on SWING, the scattering wavelength was fixed to 1.03 Å and sample-to-detector distances of 0.6 m and 6.0 m were used in order to cover a scattering wave vector (q) range from 3.0×10^{-3} to 3.5×10^{-1} $Å^{-1}$. In the case of the data recorded on XEUSS 2.0, the sample-to-detector distance was set to 2.4 m in order to cover a q range from 4.5×10^{-3} to 2.5×10^{-1} $Å^{-1}$. Samples were inserted in quartz capillaries. The raw SAXS data were corrected from the contributions induced by the capillary and the solvent (water).

The scattered intensity $I(q, r_s)$ measured for the diluted dispersions was fitted using the form factor $P_s(q, r_s)$ of polydisperse spheres for the silica nanoparticles. Fits were performed with the help of the SasView software (https://www.sasview.org). Polydisperse sphere model describes spheres with a log-normal distribution of the radius particle r_s (Eqs. 1 and 2)

$$I_{spheres}(q, r_s) = \frac{I_0}{V}[V\ (\rho_s - \rho_{solv})]^2 P_s(q, r_s) \qquad (1)$$

with

$$P_s(q, r_s) = 9\left(\frac{[\sin(qr_s) - qr_s\cos(qr_s)]}{(qr_s)^3}\right)^2 \quad (2)$$

where ρ_s and ρ_{solv} are the scattering length density of the silica nanoparticles and the solvent, respectively. For all curve the fit take onto account directly the weight of the error bat on the intensity, dI, the resolution in q of data was also take into account. The method used minimizes the χ^2, a statistical parameter that quantifies the differences between an observed data set and an expected dataset.

For concentrated solution where we cannot neglect interaction,

$$I(q) = \frac{I_0}{V}[V\ (\rho_s - \rho_{solv})]^2 P_s(q) S(q) \quad (3)$$

With S(q) the structure factor which represents the Fourier transform of center of mass position. In all cases the intensity. In different cases, all structure factors were obtained by dividing the scattered intensity by the for factor obtained for a silica solution at 1g.l^{-1} and by the volumic concentration of silica nanoparticles in solution.

Depending on the conditions of polymer adsorption and silica dispersion, the silica/PMAA dispersions were analyzed using different structure factors such as the ones given by the Hayter MSA (Means Square Approximation) and sticky hard sphere models. The Hayter MSA model calculates the interparticle structure factor for a system of charged spheres in a dielectric medium. This model has already been used for silica without PMAA.[22] Once PMAA is adsorbed onto the silica nanoparticles, we used a sticky hard sphere model which calculates the interparticle structure factor for a hard sphere fluid with a narrow, attractive, potential well.[23]

Results

1. Nanoparticles.

Silica surfaces are negatively charged at pH larger than 3 and thus a low affinity between PMAA and silica nanoparticles is anticipated in this pH range, as was observed for poly(acrylic acid) (PAA)[11], due to unfavorable electrostatic interactions. In order to modulate the interactions between PMAA and the particles, two different surface modifications of the silica nanoparticles have been performed as was described in the work by Tiraferri and coworkers.[19]

Two different alkoxysilanes were used to functionalize the nanoparticle surface. Surface functionalization of the Ludox® LS colloidal silica with (3-aminopropyl)trimethoxysilane led to introduce amine functionalities onto the surface of the nanoparticles that are henceforth referred to as $SiNH_2$ nanoparticles. The second functionalization using 3-(trimethoxysilyl)propyl-N,N,N-trimethylammonium chloride allows quaternary ammonium groups to be introduced at the silica surface and are hereafter designated as Si-TMA nanoparticles. After purification (dialysis in deionized water for 48 h), the 3 kinds of silica with the surface properties schematized on Figure 1 have been characterized using TGA and ^{13}C solid-state NMR. While TGA shows 2 additional degradation peaks (250 and 450°C) for $SiNH_2$ and Si-TMA, compared to the SiOH nanoparticles, this feature does not imply that the alkoxysilanes are indeed grafted (and not only adsorbed) on the surfaces (Figure SI1).

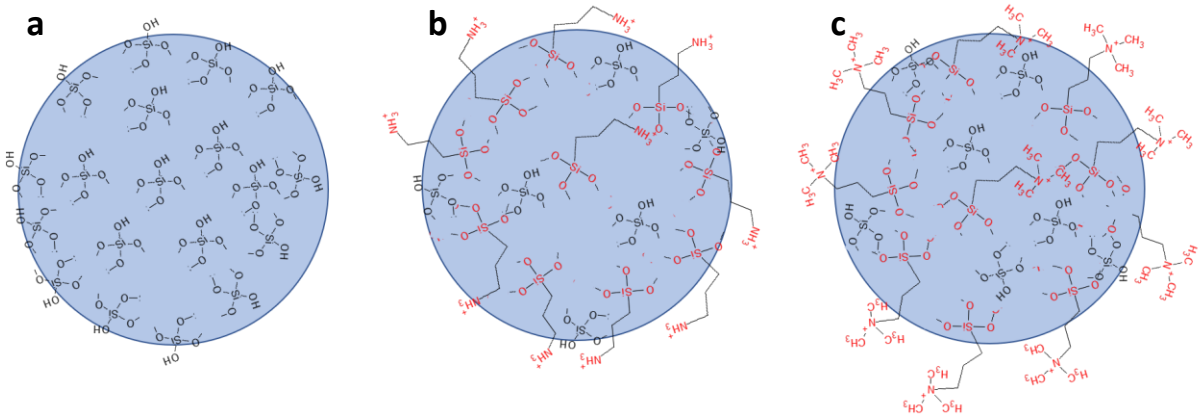

Figure 1: Schematic representation of the surface groups for SiOH (a), $SiNH_2$(b) and Si-TMA (c) nanoparticles.

Figure 2(a) shows the ^{13}C solid-state NMR spectrum obtained on both $SiNH_2$ and Si-TMA nanoparticles using a $^{1}H \rightarrow {}^{13}C$ cross-polarization (CP) experiment and a contact time of 1 ms. In the case of $SiNH_2$, the peaks at 9, 21 and 42 ppm may be assigned to the CH_2 carbon linked to the silicon atom, the intermediate CH_2 carbon ($-CH_2-\underline{C}H_2-CH_2-$) and the one linked to the nitrogen atom, respectively. Though CP does not generally lead to quantitative spectra, it is interesting to note that in this case, the area under these three peaks is very similar. This feature suggests a similar extent of the reorientational motions displayed by these CH_2 groups, leading to close values of their ^{1}H-^{13}C dipolar coupling: as a result, the resulting $^{1}H \rightarrow {}^{13}C$ CP efficiency for these CH_2 carbons is found to be comparable. Interestingly, the contribution from the methoxy carbons related to (3-aminopropyl)trimethoxysilane before reaction, usually observed

at 51 ppm in Ref. [24], was not detected in the present case, suggesting that all the OCH_3 groups were hydrolyzed and condensed with the silica surface. For the Si-TMA nanoparticles, the three methylene carbons – $N\underline{C}H_2$, $-CH_2-\underline{C}H_2-CH_2-$ and $\underline{C}H_2Si$ – give rise to the peaks at 68, 16 and 8 ppm, while the peak at 52 ppm corresponds to the $N(CH_3)_3$ carbons. Again, the areas under the peaks attributed to the CH_2 carbons are similar, which should have the same physical origin as for $SiNH_2$. In contrast, the area of the peak at 52 ppm is comparatively weaker than expected. This feature should result from the rotation of the CH_3 groups around their C_3 axis, which induces a reduction of the corresponding ^1H-^{13}C dipolar coupling and a weaker $^1H \rightarrow {}^{13}C$ CP efficiency, in comparison to the CH_2 carbons. Due to the contribution from the $N(CH_3)_3$ carbons, the possible contribution from residual methoxy carbons (δ = 51 ppm) is, in this case, more difficult to detect than for $SiNH_2$. However, the fact that the line at 52 ppm is rather symmetric suggests that the amount of unreacted OCH_3 groups, if any, should be rather weak.

Complementary ^{29}Si solid-state NMR experiments ($^1H \rightarrow {}^{29}Si$ CP) were performed on both kinds of nanoparticles, as shown in Figure 2(b). The peaks at δ = -102 ppm and -112 ppm are assigned to the Q^3 and Q^4 sites, respectively, that are already observed for the native Ludox particles. At this stage, it may be worth recalling that Q^n and T^n units correspond to $\underline{Si}(OSi)_n(OR)_{4-n}$ and $C\underline{Si}(OSi)_n(OR)_{3-n}$ species, respectively, and in the present context, ^{13}C NMR results suggest that R = H and to a far lesser extent, R = $-CH_3$. Interestingly, two additional peaks are observed at δ = -59 ppm and -69 ppm, following the grafting reactions, which indicate the occurrence of T^2 and T^3 sites. Combining these results with the ^{13}C NMR data, one may derive that alkosilanes were grafted on the silica nanoparticle surfaces, forming $Si(OSi)_2(OH)R$ and $Si(OSi)_3R$ species, where R stands for 3-aminopropyl groups ($SiNH_2$ particles) or propyl-N,N,N-trimethylammonium groups (Si-TMA particles). It should be noted that the dialysis of the particle suspensions following the silanization reactions allows to limit the proportion of by-products, such as poly(silsesquioxane)s which may potentially be formed, and therefore, supports the assignment of the solid-state NMR spectra as resulting from grafted species at the silica particle surface.

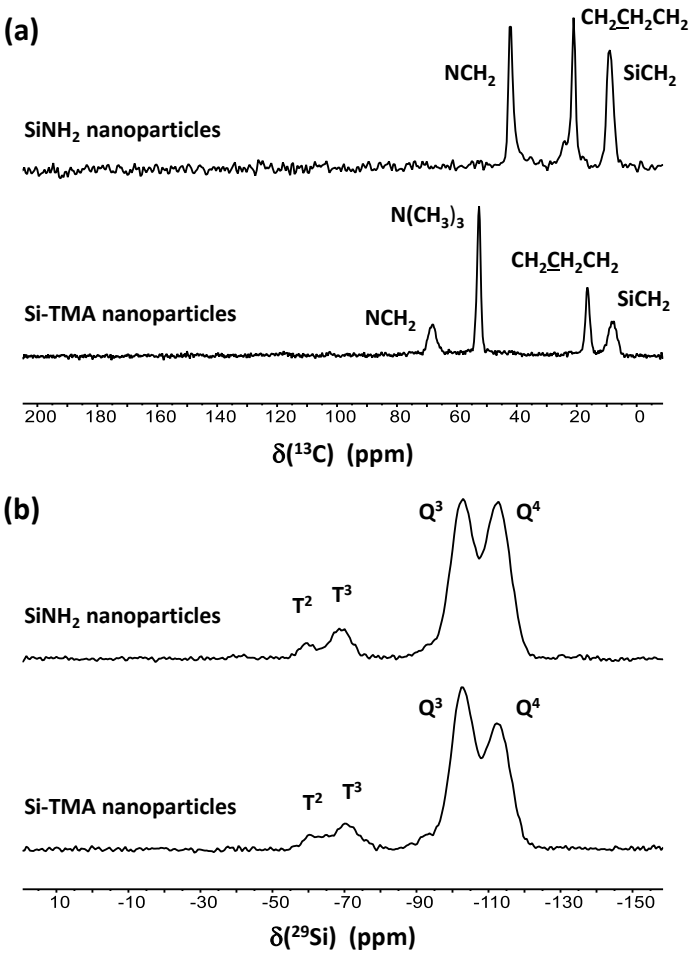

Figure 2: (a) ^{13}C and (b) ^{29}Si solid-state NMR spectra for $SiNH_2$ and Si-TMA nanoparticles. These spectra were obtained using $^{1}H \rightarrow {}^{13}C$ or $^{1}H \rightarrow {}^{29}Si$ cross-polarization.

Figure 3 shows the zeta potential (ζ) as a function of pH for dispersions of each of the nanoparticles. For the SiOH particles, ζ is slightly negative at pH = 3, close to the isoelectric point, in agreement with previous reports,[25] and it decreases as the pH increases. Such a variation corresponds to an increase of the negative surface charge density between pH = 3 and 9. At the contrary, ζ is positive in the pH range between 3 and 9 for the $SiNH_2$ nanoparticles. In this pH range, the aminopropyl groups should be protonated as the pKa of the silane reagent-(3-aminopropyl)trimethoxysilane is equal to 10.6. The protonation of the $SiNH_2$ particles is not expected to change in the pH 3 - 9 range although there is a drift of the ζ potential toward lower values, as observed for SiOH particles. Moreover, it has been reported that the amino groups interact with the silica surface via hydrogen-bonding interactions between silanolate (SiO^-) and ammonium groups ($H\text{-}NH_2^+$), which are favored by attractive electrostatic interactions.[26] Provided the grafts are chemisorbed at one extremity and physisorbed at the

other extremity, this should result in a bending of the grafts towards the silica surface and thus, an exposure of the propyl moieties to the external medium. If this process involves all, or at least, most of the grafts, the surfaces should be neutral or slightly negatively charged. Bending of part of the grafts toward the silica surface has been schematized on Figure 1b. As ζ is found to be positive in the investigated pH range (see Figure 3), one may deduce that only a part of the amino groups of the grafts should be adsorbed. For the Si-TMA nanoparticles, ζ varies quite similarly as for the $SiNH_2$ nanoparticles, except that ζ is systematically larger. The grafted alkoxysilane are now quaternized and their charge does not vary with the pH. As was mentioned for $SiNH_2$ nanoparticles, the bending of the grafts to adopt an almost flat conformation is also possible in the case of Si-TMA nanoparticles, as schematized on Figure 1c. However, the interaction of the quaternized amino groups with the silanolate cannot be due to H-bonding anymore, but only to attractive electrostatic interactions.

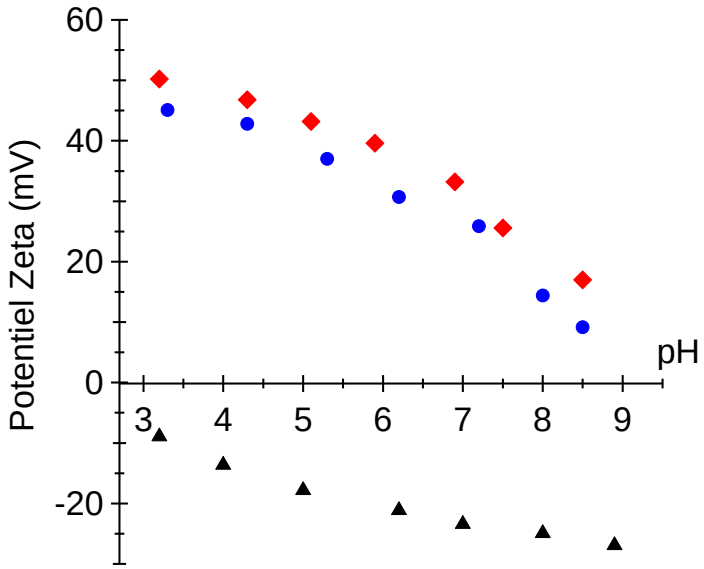

Figure 3: pH-dependence of the zeta potentials of the silica nanoparticles (2g/L) in a 0.01 M NaCl solution: SiOH (▲), $SiNH_2$ (●),Si-TMA (♦).

The structures of the SiOH and Si-TMA dispersions for different silica concentrations and pH values have been studied by SAXS (Figure 4). In the case of the SiOH nanoparticles, whatever the pH from 3 to 9, the scattered intensities at low concentration (1g/L) are well fitted by the form factor of spherical particles with an average radius R = 8 nm and a narrow (log-normal) distribution (relative standard deviation σ = 0.15), Figure SI1a. A peak is clearly observed on the structure factor when increasing the concentration from 1 to 20g/L for the dispersions at pH

= 6 and pH = 9 whereas no peak is detected at pH = 3 (Figure SI2). The structure factors have been determined by dividing the scattered intensity measured at given pH and concentration by the one determined at 1 g/L and the same pH value. An example is given on Figure SI4a at 20 g/L for pH 6 and 9 (structure factor equal to 1 at pH3). The position q* of the first maximum displayed on the structure factor evolves with the concentration according to a power law $c^{0.3}$ at pH = 6 and 9 (Figure SI4b), in good agreement with an isotropic model for dilute suspensions of particles. q* also allows the aggregation number (N_{agg}) of the nanoparticles to be determined, using the following equation:[27]

$$N_{agg} = \left(\frac{2\cdot\pi}{q^*}\right)^3 \frac{\emptyset}{V_{Si}} \quad (4)$$

ϕ denoting the volume fraction of the silica particles and V_{Si}, the volume of a particle of radius 8 nm. At 20 g/L, N_{agg} = 1.22 and 1.70 at pH = 6 and 9 respectively. Surprisingly, the nanoparticles are slightly more aggregated at pH = 9 than at pH = 6. Finally, the structure factors have been fitted by the Hayter MSA model which takes into account the surface charge of the nanoparticles.[28] The surface charge parameter of this model is an adimensional parameter representing the macroion surface charge, in number of electrons. At 20 g/L, the surface charge evolves from 20 at pH = 6 to 48 at pH = 9, clearly showing an increase of surface charges as the pH value increases. The Zeta potential decreases also when the pH is increased from 6 to 9 but the decrease is much less than the one deduced from the charge parameter. It seems that SiOH nanoparticles are forming really few aggregates which are more stable at pH 9 than at pH 6.

For the Si-TMA particles, a peak is also detected on the structure factor determined for pH ranging between 3 and 9 and at concentrations as low as 5 g/L. These structure factors have been calculated as before, by dividing the intensity by the data set measured at 1 g/L. Figure SI2b shows the intensity measurements at 1 g/L, and the fit by a polydisperse sphere model which is done with the same fit parameters as for SiOH particles. Structure factors at different concentrations and pH values have been reported on Figure SI5a. As for the SiOH particles, the concentration dependance of the position q* of the first maximum may be described by a power law $c^{0.3}$, whatever the pH value. The aggregation numbers at each pH and concentration have been reported in Table SI 1. In good agreement with ζ values, weak aggregation occurs at pH = 3 and 6 where the particles are strongly charged and stronger aggregation is observed at pH = 9 where the particles are weakly charged. The structure factors have been fitted by the Hayter

MSA model only at pH = 3 where a surface charge parameter of ~30 was obtained. In contrast, it could not be used to fit the data at pH = 9 because this model is not suited to describe weakly-charged colloids.

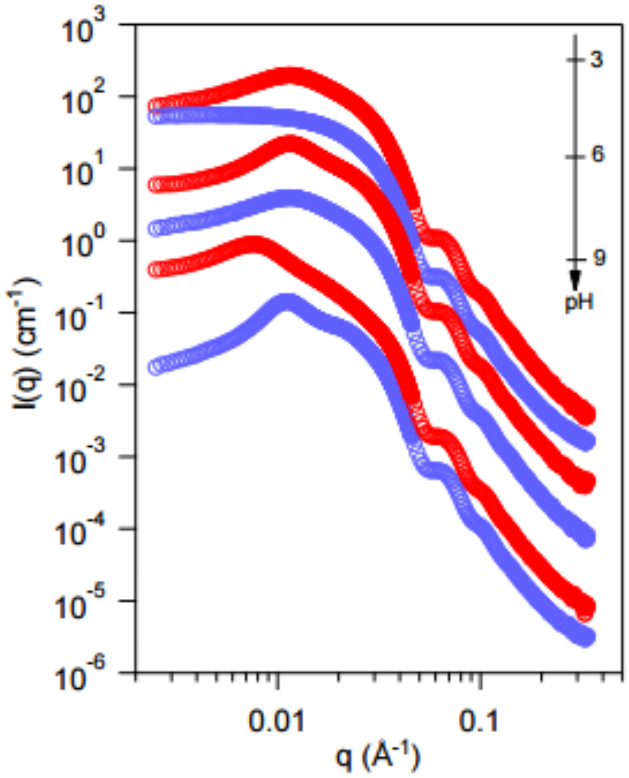

Figure 4: SAXS of SiOH (blue) and Si-TMA (red) dispersions, 20 g/L at pH = 3, 6 and 9.

2. PMAA / Silica adsorption.

Adsorption isotherms were determined on suspensions containing the same volume of solution, the same silica concentration (12.5 g/L), but various polymer concentrations. After 24 hours of equilibration under mild stirring at 20°C, the polymer content in the supernatant was analyzed by TOC and allowed the adsorbed amount to be quantified, assuming the same specific surface area (215 m^2/g) for the precursor silica nanoparticles (SiOH) and for the two surface modified particles ($SiNH_2$ and Si-TMA). The isotherms were then built for each kind of silica particles at 3 different pH values (3, 6, 9) and the results are reported on Figure 5. These data show that the pH at which adsorption takes place has a significant influence on the adsorption process. For each of the silica batches, the adsorbed amounts at saturation decrease as the pH of the solution increases. The adsorption isotherms were well fitted with a Langmuir model in the case

of the SiOH nanoparticles and at pH = 9 only for both the $SiNH_2$ and Si-TMA nanoparticles (see Table SI2 for the fit parameters). In the other cases (suspensions of $SiNH_2$ and Si-TMA at pH = 3 and 6), the isotherms are of the high affinity type, as evidenced by the sudden increase of adsorbed amounts at low concentrations which is not well fitted by a Langmuir law. This suggests stronger interactions between the polymer chains and the particles. The influence of the PMAA molar mass has been studied for Si-TMA dispersions as shown on Figure SI 6 and Table 2. A larger influence of M_w on the adsorbed amounts is observed at pH = 3 and 6, in comparison to pH = 9.

Table 2: Adsorbed PMAA amounts at saturation, Q_{sat}, for the 3 kinds of silica particles at pH = 3, 6 and 9.

Adsorbed amount at saturation, Q_{sat} (mg/m^2)	pH = 3	pH = 6	pH = 9
SiOH/PMAA1	0.18±0.02	0.14±0.02	0.10±0.02
$SiNH_2$/PMAA1	1.3 ±0.1	0.85 ±0. 2	0.5 ±0.1
Si-TMA /PMAA1	2.0 ±0.1	1.1 ±0.2	0.56 ±0.1
Si-TMA /PMAA2	1.4 ±0.1	0.83 ±0.2	0.50 ±0.1

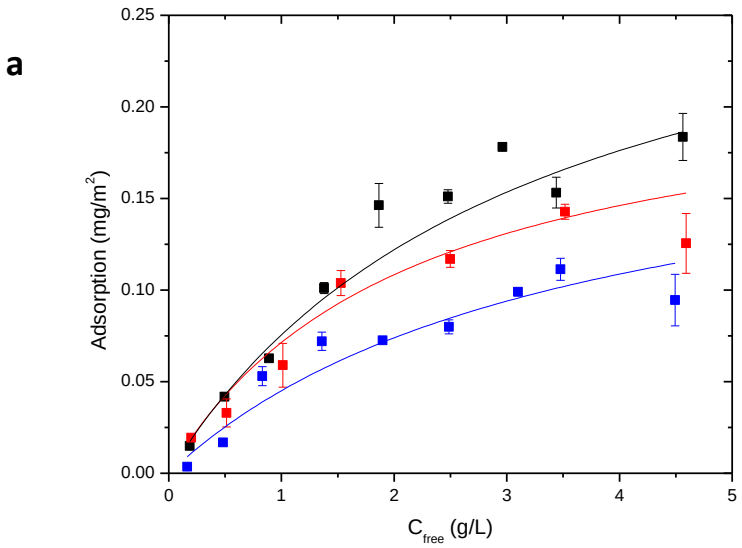

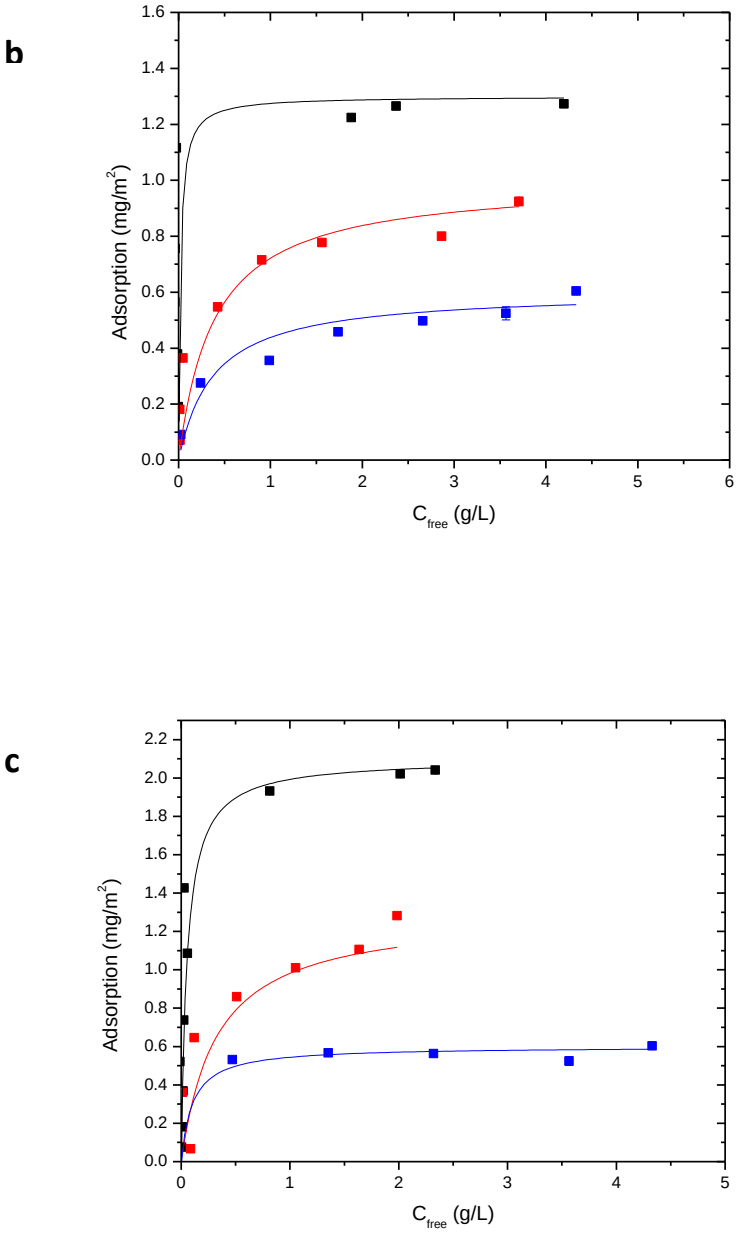

Figure 5: Adsorption isotherms of PMAA 1 on the different nanoparticles: (a) SiOH, (b) $SiNH_2$ and (c) Si-TMA. These measurements were carried out at 20°C, for pH = 3 (black), pH = 6 (red), pH = 9 (blue), using a silica concentration of 12.5 g/L. Lines correspond to fits using the Langmuir model although fits are of low quality for $SiNH_2$ and Si-TMA at low pH.

These data should be compared to literature values for the adsorption of PAA and PMAA. Adsorption of PAA onto anionic surfaces such as silica (pH above 3) shows very limited adsorbed amounts (less than 0.1 mg/m^2), which are found to get lower and lower as the pH value is increased.[11] Such a behavior can be explained by the combination of several factors

such as repulsive electrostatic interactions between polymer chains and surfaces (pH larger than 3), hydrogen bond attractive interactions (mainly at pH lower than 5) and the solvent quality of water for PAA, which evolves from theta solvent at low pH to good solvent at pH larger than 3. Adsorption of PAA onto cationic surfaces such as TiO_2,[10] mixed silica/alumina[11] or amine-functionalized silica [12] at pH = 3 results in larger adsorbed amounts, between 0.5 and 1.2 mg/m^2 typically. In all cases, the adsorbed amounts decrease as the pH value becomes higher since the surfaces are generally less positively charged and in addition, the solvent quality for PAA improves as pH increases. The PMAA adsorption behavior has been reported onto synthesized hematite particles[18] which are positively charged within the pH range 3 - 9. For a PMAA homopolymer of M_w = 75 100 g/mol, the adsorbed amount at saturation was as high as 2.1 mg/m^2 at pH = 3. It was found to display a strong reduction as the PMAA molecular weight and/or pH is increased.

Before discussing the adsorption results reported in this work, it is important to recall the conformational behavior of PMAA as a function of pH. At pH = 3, the ionization degree (α) is close to 0 and the chains adopt an hypercoiled conformation due to both intramolecular hydrogen bonds and hydrophobic interactions. As pH increases**,** the chains acquire more and more negative charges and at a critical value α_c ($\alpha_c \sim 0.22$ and pH ~ 5.5), a transition to extended random coil conformation occurs. α reaches 0.4 at pH = 6 and the chains become fully ionized at pH = 9. The coil size is known to undergo a sudden change around α_c, with almost no evolution between pH = 6 and pH = 9. At pH = 3, R_g of PMAA1 and PMAA2 have been estimated to 21.6 nm and 4.5 nm respectively from previous Rg determination by SAXS [15] on another batch and assuming a theta solvent behavior (Rg α (Mw)^1/2). It is worth noticing that these dimensions are either much larger (for PMAA1) or similar (for PMAA2) to the size of the nanoparticles ($R_{Si} \sim 8$ nm). Under these conditions, it is not totally justified to deal about adsorption of PMAA onto silica nanoparticles but more to PMAA/silica nanoparticle interactions. However, the discussion in terms of adsorbed amounts of PMAA is maintained for the sake of convenience. From the adsorbed amounts at saturation Q_{sat} (see Table 2), it is possible to estimate the number of adsorbed chains per silica particle at saturation, N_{ads}, from the following expression:

$$N_{ads} = (4\pi \times N_a/M_n) \times R_{Si}^2 \times Q_{sat} \quad (5)$$

M_n denoting the number average molar mass of the polymer and N_a, the Avogadro number. The N_{ads} values are found to be low (less than 0.2) in the case of SiOH nanoparticles. On average,

5 to 10 particles interact with a single chain. The SAXS results, which will be reported below, will allow to discriminate between these two situations. In the case of $SiNH_2$ and Si-TMA particles, N_{ads} is close to unity except at pH = 9, for which values around 0.5 are obtained. In the case of the PMAA chains with a lower Mw value (PMAA2), much more than one chain interact with any Si-TMA silica particle. At pH = 3, for which the chains adopt an hypercoiled conformation, N_{ads} (≈ 33 chains per particle) is in good agreement with the one estimated by assuming a full surface coverage of silica nanoparticles, characterized by a radius of 8 nm, with PMMA coils displaying a radius of 4.5 nm (≈ 31 chains per particle).

One may attempt to correlate the adsorption behavior observed for the different kinds of silica particles, at the three pH values, to the possible interaction mechanisms. The main interaction involved in the case of SiOH/PMAA is of electrostatic nature. SiOH nanoparticles are indeed negatively charged over the whole pH range investigated. PMAA is neutral at pH = 3 or negatively charged at higher pH values. Therefore, electrostatic interactions should then be either non-efficient (pH = 3) or repulsive (pH > 3). Hydrogen bond interactions could take place between the silanol surface sites and the carboxylic acid groups of PMAA. However, at low pH, these interactions may be neglected compared to the strong intramolecular H-bonds within PMAA hypercoils. For pH above 6, intramolecular interactions within PMAA coils are not dominant anymore whereas hydrogen bonds with the silica surface sites are less and less possible as both carboxylic acid and silanol groups are increasingly deprotonating as pH is raised up. Such considerations explain why the interactions of PMAA with the SiOH nanoparticles are very weak and get more and more reduced with pH.

At first glance, the results obtained for both $SiNH_2$ and Si-TMA nanoparticles may seem to be counterintuitive. Both nanoparticles are indeed strongly positively charged at pH = 3 and 6 while the higher adsorbed amounts are observed at pH = 3, for which the polymer chains are not charged. In fact, such a behavior may be rationalized by taking into account the additional hydrophobic interactions related to the grafts at the silica surface. In the case of $SiNH_2$, the hydrophobicity of the surface is enhanced due to the propyl moieties. Moreover, it has been shown that part of the grafted aminopropyl groups could form loops,[26] thus exposing them to the solution (see Figure 1). At the same time, the PMAA hypercoils displayed at pH = 3 are exposing their methyl groups. As a result, the higher extent of PMAA adsorption at pH = 3, compared to pH = 6, could be mainly attributed to hydrophobic interactions between the coils and the $SiNH_2$ silica surface. At larger pH values, the PMAA conformations are less coiled, the hydrophobic interactions should get weaker while the electrostatic attractive interactions take

place at pH = 6 and, at a lower extent, at pH = 9 where the SiNH2 surfaces are less charged. The Si-TMA /PMAA interaction mechanisms should be quite similar to the ones involved for $SiNH_2$/PMAA. The main difference stands in the higher hydrophobicity of the Si-TMA surfaces due to the quaternization of the ammonium groups and thus implies stronger hydrophobic interactions. This feature should account for the larger adsorbed amounts observed for these suspensions at pH = 3 and 6 (see Figure 5(b) and Figure 5(c)).

3. SAXS study of the silica/PMAA dispersions.

All the samples considered for the SAXS experiments have been prepared under the same conditions as the ones used for the adsorption studies. Besides, the silica and polymer concentrations (12.5 g/L and 4 g/L, respectively) were chosen so that the PMMA chain adsorption has achieved the saturation regime for almost all the dispersions. SAXS data should allow to deduce informations about the dispersion state of the aggregates. Indeed, a dispersed state is considered as a one where aggregates of finite sizes are dispersed in the solution and show a good stability: too large and/or dense aggregates should sediment and introduce phase separation. Thus a plateau in the low q domain is indicative of the formation of aggregates of sizes lower than 100 nm. Conversely, when there is no plateau but a power low behavior q^{-x} at low q, this should mean that aggregates larger than 100 nm (compacity related to x values) are formed.

The intensities scattered by SiOH/PMAA dispersions have been reported on Figure 6(a). Due to the scattering contrasts of X-ray radiation and the silica concentration of the samples, the signal mostly results from the silica nanoparticles, and not from PMAA. The results were fitted by a model describing the homogeneous dispersion of spheres, corresponding to silica nanoparticles of radius 79 Å. It can be seen that the scattered intensity profiles are the same for all pH values and differ only slightly from the form factor of a hard sphere. The Hayter MSA model, previously used for dispersions of neat SiOH particles at pH 6 and 9, was again considered in this case. As mentioned earlier, it takes into account the surface charge of the nanoparticles and in the present case, it could not be used suggesting weakly charged colloids at the three pH, in contrast to the results obtained with neat SiOH particles at pH 6 and 9.

As previously reported in the first part of this work, the functionalization at the silica surface results in a higher amount of adsorbed PMMA chains. Therefore, it is of interest to investigate whether such a stronger adsorption may influence the silica dispersions. For the $SiNH_2$/PMAA

dispersions, a little aggregation of silica nanoparticles at pH = 6 and pH = 9 is observed. The SAXS data shown in Figure 6b could indeed be fitted by a sticky hard sphere model, with an aggregation number equal to 2 for both pH values. χ^2 obtained for pH 6 and 9 are respectively equal to 55 and 65. At pH = 3 a phase separation occurs. The volume fraction of the lower phase is rather low so that it was impossible to measure its SAXS signal. The profile presented on Figure 6b is the one collected from the upper phase obtained at pH = 3. It is obvious that silica nanoparticles are still present but at a lower concentration in this phase (concentration divided by 2, calculated from rescaling on the secondary speak domain 0.06-0.07 $Å^{-1}$). At low q values, I(q) displays a power law dependence with a slope 2.7 which is characteristic of a fractal dispersion of silica nanoparticles.[29] Aggregates of fractal dimension 2.7 should be formed but their size could not be determined as no plateau was attained at the lowest q value accessed (0.003 $Å^{-1}$).

The scattered intensities collected from the Si-TMA /PMAA dispersions are fh pH value. At pH = 9, as already observed for $SiNH_2$/PMAA, the nanoparticles were well dispersed. The SAXS profile from such silica dispersions could be fitted by a sticky hard sphere model. χ^2 is equal to 53. The resulting fitting parameters suggest that the silica nanoparticles were slightly aggregated, with an aggregation number N_{agg} = 6. At pH = 6 and 3, completely different dispersion states were observed, since phase separations occur. At pH = 6, the phase separation is not visible to the eye but the SAXS intensity in the range q = 0.06 – 0.07 $Å^{-1}$, which is related to the first peak of the form factor for spherical nanoparticles, decreased by a factor 1.8. As the intensity I(q) is proportional to the silica concentration, this means that the silica concentration in the analyzed part of the sample is 1.8 times lower than its nominal value (12.5 g/L). Consequently, phase separation must have occurred and a phase with a small volume characterized by a larger silica concentration should be present at the bottom of the sample. In the analyzed phase (upper phase), a clear silica aggregation can be deduced from the evolution of I(q) in the low-q range . This latter indeed shows a power law dependence, $I(q) \propto q^{-3.2}$, indicating the formation of dense silica aggregates. Moreover, the peak at 0.040 $Å^{-1}$ is related to a characteristic distance between silica nanoparticles of 157 Å. As the radius of one silica particle is 79 Å, it implies that silica nanoparticles are in contact with each other within the aggregates. At pH = 3, a clear phase separation is observed at the macroscopic length scale. The SAXS profile measured in the upper phase is not represented here but the intensity I(q) was almost flat, revealing the absence of silica nanoparticles. The results obtained for the lower phase again reveal the presence of dense aggregates formed by the silica nanoparticles, with a

higher concentration than the nominal one. As for the sample at pH = 6, the peak at 0.040 $Å^{-1}$ indicates that the characteristic distance between nanoparticles within the aggregates is 158 Å.

At this stage, it is important to correlate the results of the SAXS measurements to the silica/PMAA interactions. Adding polymer chains to silica dispersions may influence their morphology in several ways, as a result of additional particle/particle interactions such as steric stabilization, screened electrostatic interactions, depletion or bridging.[10, 30, 31, 32] It should be outlined that thanks to the large contour length of PMAA chains (1.3 μm) compared to the radius of silica nanoparticles (79 Å), bridging interactions may possibly occur. In order to discriminate the interactions at play in the different conditions, the concentration of free PMAA chains (C_{free}) and the number of PMAA chains interacting with one silica nanoparticle ($N_{ads/particle}$) have been calculated from the adsorption isotherms, for each SAXS sample. The results are summarized in Table 3, together with the dispersion state of the silica nanoparticles for each sample. For the SiOH/PMAA samples, it has been shown that the polymer/particle interactions are very weak. Consequently, the number of PMAA chains interacting with one nanoparticle stands well below 1 (ranging from 0.1 to 0.25) and thus polymer adsorption should not lead to nanoparticle aggregation by bridging. At pH = 3, the free PMAA chains (3.5 g/L) could promote aggregation by depletion but this is not the case as the SiOH/PMAA sample shows the same scattering profile as a SiOH dispersion in water, at similar concentrations (Figure 4) for which the silica nanoparticles are perfectly dispersed. Unlike pH = 3, the SiOH and SiOH/PMAA samples behave differently at pH = 6 and 9. A repulsive structure factor is clearly detected on the SAXS data of SiOH dispersions (Figure 4 and Figure 3), which can be attributed to electrostatic repulsion of the charged silica nanoparticles at these pH values. At the contrary, no structure factor is detected for the SiOH/PMAA samples (pH = 6 and 9) for which the SAXS profiles are almost perfectly superimposed on the one of SiOH/PMAA at pH = 3. Electrostatic repulsions between the nanoparticles are obviously screened at these pH values. Table 3 shows that free PMAA chains are essentially present in the samples with concentrations close to the nominal concentration of 4 g/L. Their free counter ions could contribute to the screening of the electrostatic repulsions between nanoparticles at pH = 6 and pH = 9 (PMAA chains are almost uncharged at pH = 3). Taking into account the different ionization degrees and the Manning condensation at pH = 6 and 9, the values of the Debye length (λ_D) estimated were similar for the two pH values, around 3.5 nm. The average distance D between non-aggregated nanoparticles may be estimated to $2R_{silica} \times (d/C_{silica})^{1/3}$ where d denotes the density of silica (2.2), C_{silica} = 12.5 g/L, R_{silica} = 79 Å. Therefore, D amounts to 87

nm, which is much larger than λ_D. The free counterions of the free PMAA chains thus contribute efficiently to the screening of the electrostatic repulsions between silica nanoparticles and this explains the results obtained at pH = 6 and 9.

PMAA adsorbs to a larger extent onto the positively-charged $SiNH_2$ nanoparticles than onto SiOH (adsorbed amounts 5 to 7 times weaker at the saturation plateau). At pH = 3, a single $SiNH_2$ nanoparticle interacts on average with more than one PMAA chain (1.7) and thus networks of nanoparticles connected through polymer bridges could be formed. Such a strong attractive interaction between the nanoparticles may result in the phase separation observed. Large fractal aggregates detected in the upper phase are also indicative of these attractive interactions induced by the polymer chains. At pH = 6 and 9, the adsorbed amounts of PMAA are lower than the one at pH = 3 so that each nanoparticle interacts on average with no more than one PMAA chain, preventing the formation of large aggregates. Thus, in agreement with the adsorption behavior, low aggregation numbers were found by SAXS (N_{agg} =2). Adsorption of negatively-charged PMAA chains onto positively-charged nanoparticles may indeed partly screen the electrostatic repulsions between nanoparticles. Besides, as for SiOH/PMAA, the presence of free PMAA chains in the dispersions should also contribute to the screening of electrostatic interactions. The Debye length associated to the free counter-ions ranges between 4 nm (pH = 9) and 5 nm (pH = 6), which is much lower than the average distance between slightly aggregated silica nanoparticles (109 nm). Both interactions account for the absence of structure factors at pH = 6 and 9.

PMAA adsorbs more strongly onto the Si-TMA nanoparticles than onto the $SiNH_2$ nanoparticles which are both negatively-charged. At pH = 3 and pH = 6, the number of adsorbed chains per nanoparticle is bigger than one, allowing the formation of networks of nanoparticles connected by PMMA chains. In good correlation with these adsorption results, phase separations are observed for these two samples. It should be noted that the plateau of adsorption was not reached at pH = 3 under the conditions of the experiments. Indeed, the PMAA1 concentration (4 g/L), is too low to reach the adsorbed amount at saturation (2 mg/m^2, Table 2). The partial surface coverage of the Si-TMA particles, estimated as the ratio of the actual adsorbed amount (1.38 mg/m^2) to the one at the plateau value is 0.68. As the surfaces are able to adsorb 32% more, this could induce additional bridging interactions between the uncovered surface patches and some dangling portions of adsorbed chains. Indeed, the phase separation was more clearly observed at pH = 3, for which all the silica nanoparticles settled in the lower phase. At pH = 9, the adsorbed amount of PMAA chains is lower than in the case of pH = 3 and

similar to the one obtained for $SiNH_2$, with a number of chains adsorbed per nanoparticle of 0.6. This feature should prevent the formation of large aggregates. Indeed, the formation of small aggregates with $N_{agg} = 6$ was deduced from the SAXS experiments. Moreover, at this pH, the presence of free chains should favor the screening of electrostatic interactions, as the Debye length associated with the free counter-ions is 4.2 nm, which is much lower than the average distance between slightly aggregated silica nanoparticles (157 nm).

Table 3: Characteristics of the silica/PMAA dispersions (12.5 g/L for silica, 4 g/L for PMAA1) investigated by SAXS. C_{free} (g/L) and $N_{ads/particle}$ denote, respectively, the concentration of free PMAA chains and the number of PMAA chains interacting with one nanoparticle, as deduced from Table 2. The various dispersion states of the silica particles are derived from the analysis of the SAXS data. *: This sample is not at the adsorption saturation.

Silica/PMAA1 samples		pH = 3	pH = 6	pH = 9
SiOH	C_{free} (g/L)	3.5	3.6	3.7
	$N_{ads/particle}$	0.24	0.18	0.13
	Dispersion state	Dispersed: non-aggregated	Dispersed: non-aggregated	Dispersed: non-aggregated
$SiNH_2$	C_{free} (g/L)	0.5	1.7	2.7
	$N_{ads/particle}$	1.7	1.1	0.6
	Dispersion state	Phase separated: Upper phase: fractal aggregates	Dispersed: $N_{agg} = 2$	Dispersed: $N_{agg} = 2$
Si-TMA	C_{free} (g/L)	~ 0	1.0	2.5
	$N_{ads/particle}$	1.8 *	1.4	0.7
	Dispersion state	Phase separated: Lower phase: compact aggregates	Phase separated: Upper phase: compact aggregates	Dispersed: $N_{agg} = 6$

a

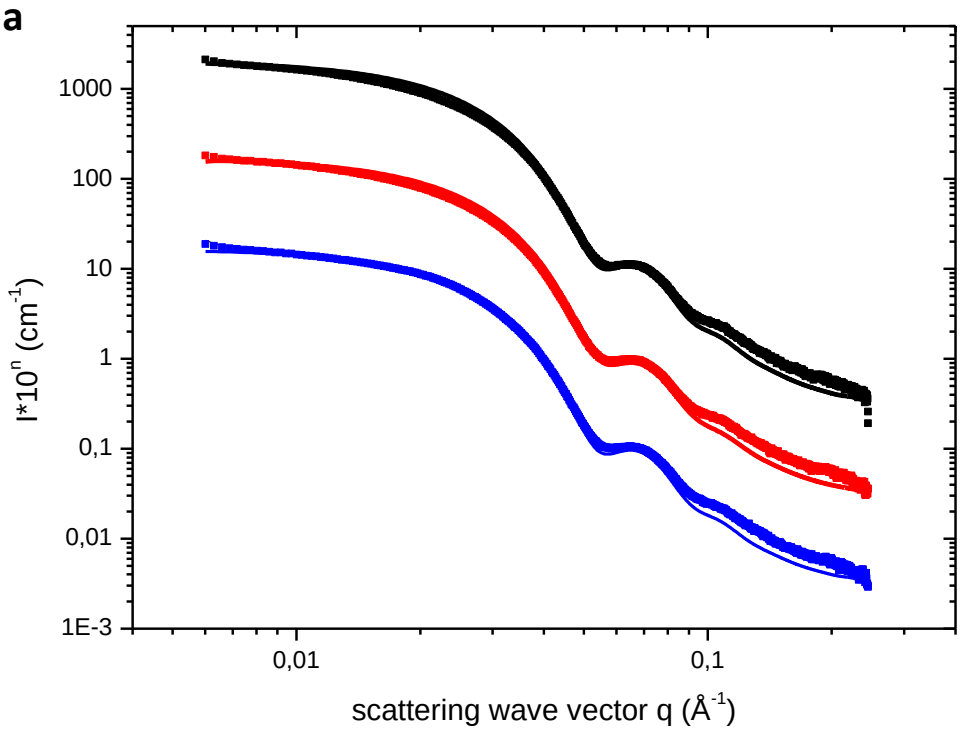
1000
100
10
1
0,1
0,01
1E-3
0,01
0,1
I*10^n (cm^-1)
scattering wave vector q (Å^-1)

b

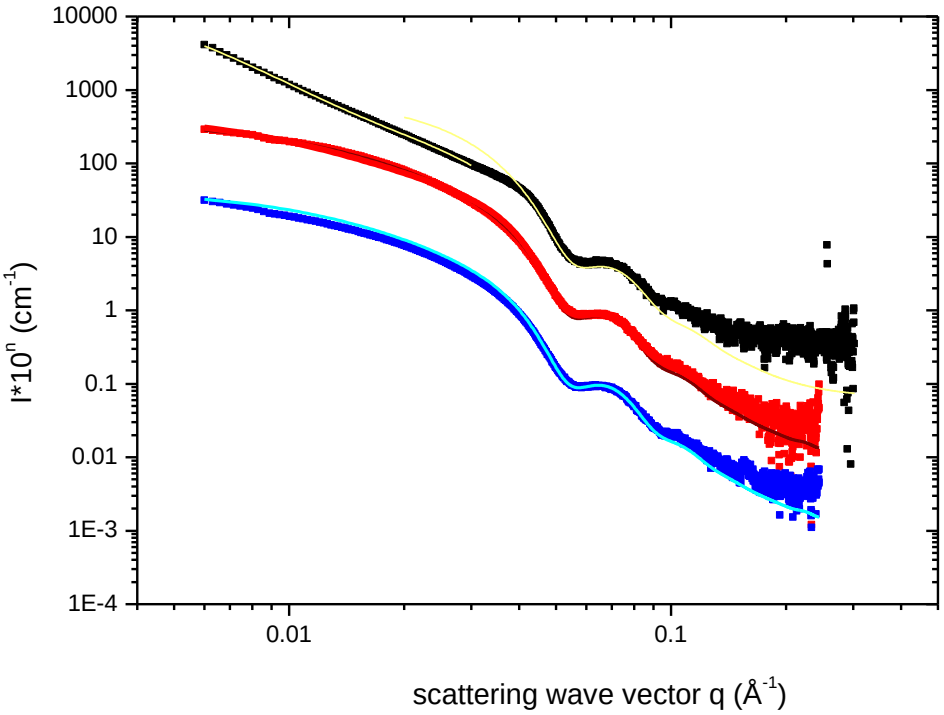
10000
1000
100
10
1
0.1
0.01
1E-3
1E-4
0.01
0.1
I*10^n (cm^-1)
scattering wave vector q (Å^-1)

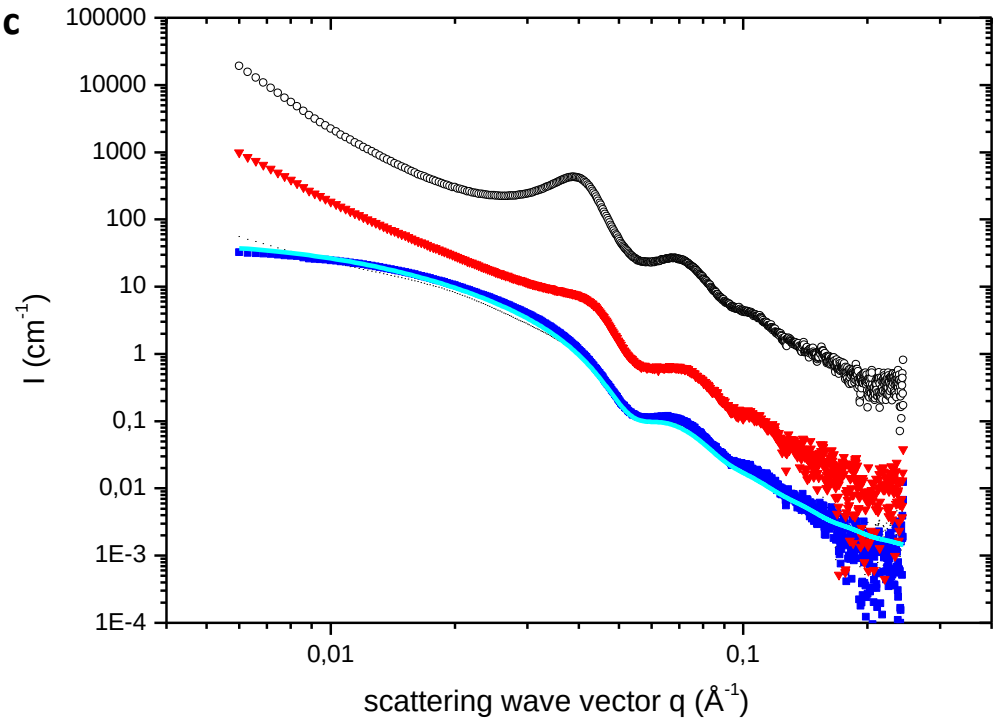

Figure 6: SAXS profiles of silica dispersions (12.5 g/L) in the presence of PMAA1 (4 g/L) at pH = 3 (black), pH = 6 (red), pH = 9 (blue). For each nanoparticle, the curves have been vertically translated by a factor 10^n for clarity. (a) SiOH/PMAA1 dispersions. The solid lines stand for the fits of the experimental data by a model of homogeneous sphere dispersions. (b) $SiNH_2$ /PMAA1 dispersions. The data have been fitted using the sticky hard sphere dispersion model. (c) Si-TMA /PMAA1 dispersions. The fitting line was deduced based on the sticky hard sphere dispersion model.

Conclusion

In this work, it was shown that the PMAA/silica interactions can be tuned either by the pH or by the surface modification of the silica nanoparticles. The native silica nanoparticles (SiOH) interact only weakly with PMAA and this interaction tends to vanish as the pH value decreases. Stronger interactions were evidenced for amine-functionalized silica nanoparticles ($SiNH_2$ and Si-TMA). At low pH for which PMAA is uncharged, these strong interactions are mainly of hydrophobic nature between the propyl moieties of the grafts at the silica surfaces and the methyl groups of the PMAA hypercoils. At higher pH, the adsorption is mainly driven by

electrostatic interactions between positively-charged surfaces and negatively-charged PMAA chains. These interactions are weaker than at pH 3 and decrease as pH is raised up.

Silica nanoparticle self-assembly strongly depends on the polymer/silica surface interactions. The adsorbed PMAA chains may develop several kinds of interactions –steric repulsion, bridging attraction~~,~~ – while the free non-adsorbing chains are also at play with possible depletion attraction or electrostatic screening. Under the conditions investigated in this work (mostly saturation adsorption), the main parameter governing the occurrence of aggregation is the average number of PMAA chains interacting with one silica nanoparticle. If this number is higher than one, bridging interactions dominate and lead to phase separations with the formation of large silica aggregates. At the contrary, if this number is lower than one, bridging interactions are not the governing ones and the silica dispersions are stable with low aggregation numbers. Thus, a fine tuning of the polymer/silica interactions may allow tailorable stability of colloidal systems to be achieved.

Acknowledgements:

The authors acknowledge late Solomanpionona Randriamahefa for his help in polymer modification

Funding:

This work was supported by the LABEX MMCD.

References

1. Bolto, B. & Gregory, J. Organic polyelectrolytes in water treatment. *Water Res.* **41**, 2301–2324 (2007).
2. Chen, X., Huang, R. & Pelton, R. The Reinforcement of Calcium Carbonate Filled Papers with Phosphorus-Containing Polymers. *Ind. Eng. Chem. Res.* **44**, 2078–2085 (2005).
3. Luo, K. *et al.* Self-Assembly of SiO₂/Gd-DTPA-Polyethylenimine Nanocomposites as Magnetic Resonance Imaging Probes. *J. Nanosci. Nanotechnol.* **10**, 540–548 (2010).
4. Trantakis, I. A., Bolisetty, S., Mezzenga, R. & Sturla, S. J. Reversible Aggregation of DNA-Decorated Gold Nanoparticles Controlled by Molecular Recognition. *Langmuir* **29**, 10824–10830 (2013).
5. Guo, J., Yang, W. & Wang, C. Magnetic Colloidal Supraparticles: Design, Fabrication and Biomedical Applications. *Adv. Mater.* **25**, 5196–5214 (2013).
6. Forsman, J. Polyelectrolyte Adsorption: Electrostatic Mechanisms and Nonmonotonic Responses to Salt Addition. *Langmuir* **28**, 5138–5150 (2012).
7. Szilagyi, I., Trefalt, G., Tiraferri, A., Maroni, P. & Borkovec, M. Polyelectrolyte adsorption, interparticle forces, and colloidal aggregation. *Soft Matter* **10**, 2479–2502 (2014).
8. Van de Steeg, H. G. M., Cohen Stuart, M. A., De Keizer, A. & Bijsterbosch, B. H. Polyelectrolyte adsorption: a subtle balance of forces. *Langmuir* **8**, 2538–2546 (1992).
9. Dobrynin, A. & Rubinstein, M. Theory of polyelectrolytes in solutions and at surfaces. *Prog. Polym. Sci.* **30**, 1049–1118 (2005).
10. Liufu, S., Xiao, H. & Li, Y. Adsorption of poly(acrylic acid) onto the surface of titanium dioxide and the colloidal stability of aqueous suspension. *J. Colloid Interface Sci.* **281**, 155–163 (2005).
11. Wiśniewska, M., Urban, T., Grządka, E., Zarko, V. I. & Gun'ko, V. M. Comparison of adsorption affinity of polyacrylic acid for surfaces of mixed silica–alumina. *Colloid Polym. Sci.* **292**, 699–705 (2014).

12. Joksimovic, R., Prévost, S., Schweins, R., Appavou, M.-S. & Gradzielski, M. Interactions of silica nanoparticles with poly(ethylene oxide) and poly(acrylic acid): Effect of the polymer molecular weight and of the surface charge. *J. Colloid Interface Sci.* **394**, 85–93 (2013).
13. Moussaid, A., Schosseler, F., Munch, J. P. & Candau, S. J. Structure of polyacrylic acid and polymethacrylic acid solutions : a small angle neutron scattering study. *J. Phys. II* **3**, 573–594 (1993).
14. Mandel, M., Leyte, J. & Stadhouder, M. The Conformational Transition of Poly(methacrylic acid) in Solution. *J. Phys. Chem.* **71**, 603–612 (1967).
15. Robin, C. *et al.* Unexpected Rheological Behavior of Concentrated Poly(methacrylic acid) Aqueous Solutions. *Macromolecules* **50**, 700–710 (2017).
16. Morawetz, H. Revisiting some phenomena in polyelectrolyte solutions. *J. Polym. Sci. Part B Polym. Phys.* **40**, 1080–1086 (2002).
17. Ruiz-Pérez, L. *et al.* Conformation of Poly(methacrylic acid) Chains in Dilute Aqueous Solution. *Macromolecules* **41**, 2203–2211 (2008).
18. Chibowski, S., Patkowski, J. & Grządka, E. Adsorption of polyethyleneimine and polymethacrylic acid onto synthesized hematite. *J. Colloid Interface Sci.* **329**, 1–10 (2009).
19. Tiraferri, A., Kang, Y., Giannelis, E. P. & Elimelech, M. Highly Hydrophilic Thin-Film Composite Forward Osmosis Membranes Functionalized with Surface-Tailored Nanoparticles. *ACS Appl. Mater. Interfaces* **4**, 5044–5053 (2012).
20. Couvreur, L. *et al.* First Nitroxide-Mediated Controlled Free-Radical Polymerization of Acrylic Acid. *Macromolecules* **36**, 8260–8267 (2003).
21. Delgado, A. V., González-Caballero, F., Hunter, R. J., Koopal, L. K. & Lyklema, J. Measurement and Interpretation of Electrokinetic Phenomena (IUPAC Technical Report). *Pure Appl. Chem.* **77**, 1753–1805 (2005).
22. Hayter, J. B. & Penfold, J. An analytic structure factor for macroion solutions. *Mol. Phys.* **42**, 109–118 (1981).

23. Rao, K. S. *et al.* Small angle neutron scattering from micellar solutions of triton X-100. *Pramana* **37**, 311–319 (1991).

24. Radi, S. *et al.* Organically Modified Silica with Pyrazole-3-carbaldehyde as a New Sorbent for Solid-Liquid Extraction of Heavy Metals. *Molecules* **19**, 247–262 (2013).

25. Iler, R. K. *The chemistry of silica: solubility, polymerization, colloid and surface properties, and biochemistry*. (Wiley, 1979).

26. Chiang, C.-H., Ishida, H. & Koenig, J. L. The structure of γ-aminopropyltriethoxysilane on glass surfaces. *J. Colloid Interface Sci.* **74**, 396–404 (1980).

27. Oberdisse, J. Aggregation of colloidal nanoparticles in polymer matrices. *Soft Matter* **2**, 29–36 (2006).

28. Hansen, J.-P. & Hayter, J. B. A rescaled MSA structure factor for dilute charged colloidal dispersions. *Mol. Phys.* **46**, 651–656 (1982).

29. Teixeira, J. Small-angle scattering by fractal systems. *J. Appl. Crystallogr.* **21**, 781–785 (1988).

30. Genix, A.-C. & Oberdisse, J. Nanoparticle self-assembly: from interactions in suspension to polymer nanocomposites. *Soft Matter* **14**, 5161–5179 (2018).

31. Shi, L., Carn, F., Boué, F., Mosser, G. & Buhler, E. Control over the electrostatic self-assembly of nanoparticle semiflexible biopolyelectrolyte complexes. *Soft Matter* **9**, 5004 (2013).

32. Li, F., Sun, D., Wu, T. & Li, Y. Aggregation and deposition of in situ formed colloidal particles in the presence of polyelectrolytes. *Soft Matter* **13**, 1539–1547 (2017).